Table 2.5.3.15. *Pentagonal and decagonal point groups constructed by analogy with trigonal and hexagonal point groups*

This table is taken from Saito *et al.* (1992) with the permission of the Japan Society of Applied Physics.

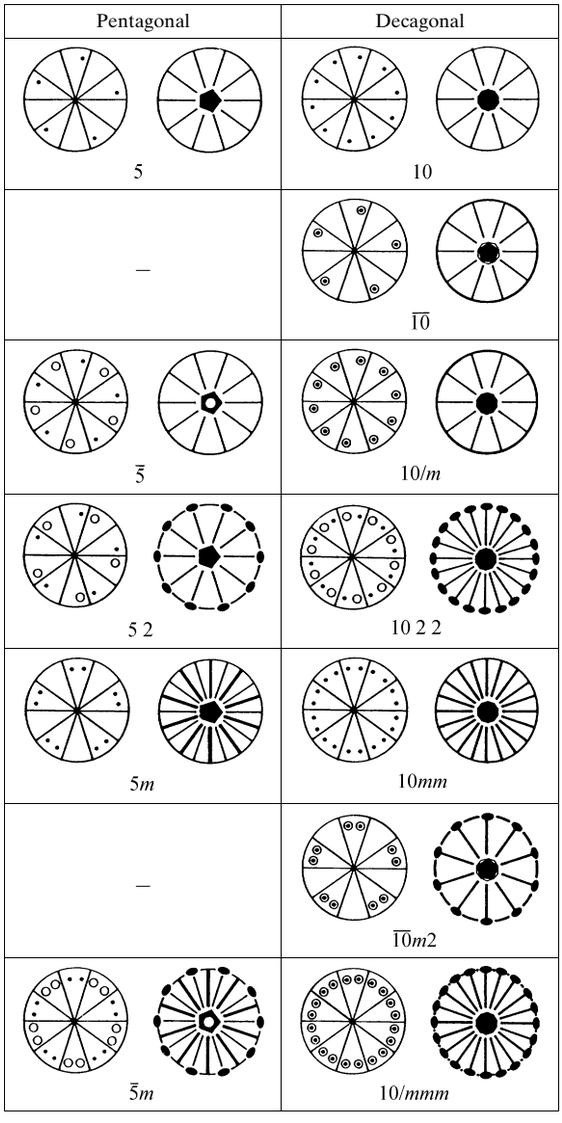

10*mm*. The whole pattern of Fig. 2.5.3.24(*b*), formed by HOLZ reflections, shows a fivefold rotation symmetry and a type of mirror plane, the resultant symmetry being 5*m*. Figs. 2.5.3.24(*c*) and (*d*) show symmetries 6*mm* and 3*m*, respectively. Figs. 2.5.3.24(*e*) and (*f*) show symmetry 2*mm*. There are two icosahedral point groups, 235 and $m\bar{3}\bar{5}$ (see Table 10.1.4.3 in *IT* A, 2005). The former is noncentrosymmetric with no mirror symmetry but the latter is centrosymmetric. Table 2.5.3.14 shows the diffraction groups expected from these point groups with the incident beam parallel to the fivefold or tenfold axis, and their symmetries appearing in the WP, BP, DP and ±DP. Projection diffraction groups and their symmetries, in which only the interaction between ZOLZ reflections is taken into account, are given in the second row of each pair. Diffraction groups obtained for the other incident-beam directions are omitted because they can be seen in Table 2.5.3.3. The whole-pattern symmetries observed for better-quality images of $Al_{74}Mn_{20}Si_6$ have confirmed the result of Bendersky & Kaufman (1986), *i.e.* the point group $m\bar{3}\bar{5}$. Fig. 2.5.3.25(*a*) shows a zone-axis CBED pattern taken at an electron incidence along the threefold axis. Figs. 2.5.3.25(*b*) and (*c*) show ±DPs taken when tilting the incident beam to excite a low-order strong reflection. The pattern of disc $+G$ agrees with that of disc $-G$ when the former is superposed on the latter with a translation of $-2G$. This symmetry 2_R directly proves that the quasicrystal is centrosymmetric, again confirming the point group as $m\bar{3}\bar{5}$. The lattice type was found to be primitive and no dynamical extinction was observed. Thus, the space group of the alloy was determined to be $Pm\bar{3}\bar{5}$.

Quasicrystals of Al–Mn alloys have been produced by the melt-quenching method and are thermodynamically metastable. Tsai *et al.* (1987) discovered a stable icosahedral phase in $Al_{65}Cu_{20}Fe_{15}$. This alloy has larger grains and is much better quality with less phason strain than $Al_{74}Mn_{20}Si_6$. The discovery of this alloy greatly accelerated the studies of icosahedral quasicrystals. It was found that the lattice type of this phase and of some other Al–Cu–TM (TM = transition metal) alloys is different from that of Al–Mn alloys. That is, Al–Cu–TM alloys display many additional spots in diffraction patterns of twofold rotation symmetry. The patterns were indexed either by all (six) even or all (six) odd, or by a face-centred (*F*) lattice. All the icosahedral quasicrystals known to date belong to the point group $m\bar{3}\bar{5}$; none with the noncentrosymmetric point group 235 have been discovered.

2.5.3.5.2. Decagonal quasicrystals

The first decagonal quasicrystal was found by Bendersky (1985) in an alloy of Al–Mn using the electron-diffraction technique. This phase has periodic order parallel to the tenfold axis, like ordinary crystals, but has quasiperiodic long-range structural order perpendicular to the tenfold axis. The diffraction peaks were indexed by one vector parallel to the tenfold axis and four independent vectors pointing to the vertices of a decagon. Thus, the decagonal quasicrystal is described in terms of a regular crystal in five dimensions.

Two space groups, $P10_5/m$ and $P10_5/mmc$, have been proposed for the alloy by Bendersky (1986) and by Yamamoto & Ishihara (1988), respectively. However, owing to the low quality of the specimens, CBED examination of the alloy could not determine whether the point group is 10/*m* or 10/*mmm*. Furthermore, identification of the space-group symmetry was not possible because observation of dynamical extinction caused by the screw axis and/or the glide plane was difficult. The Al–*M* (*M* = Mn, Fe, Ru, Pt, Pd, ...) quasicrystals found at an early stage were thermodynamically metastable. Subsequently, thermodynamically stable decagonal phases were discovered in the ternary alloys $Al_{65}Cu_{15}Co_{20}$ (Tsai *et al.*, 1989*a*), $Al_{65}Cu_{20}Co_{15}$ (He *et al.*, 1988) and $Al_{70}Ni_{15}Co_{15}$ (Tsai *et al.*, 1989*b*). However, space-group determination was still difficult due to their poor quasicrystallinity.

Tsai *et al.* (1989*c*) succeeded in producing a metastable but good-quality decagonal quasicrystal of $Al_{70}Ni_{15}Fe_{15}$. This alloy was found to be the first decagonal quasicrystal that could tolerate symmetry determination using CBED. The space group was determined to be $P\bar{1}0m2$ by Saito *et al.* (1992).

Fig. 2.5.3.26(*a*) shows a CBED pattern of $Al_{70}Ni_{15}Fe_{15}$ taken with an incidence parallel to the fivefold axis (*c* axis). The pattern clearly exhibits fivefold rotation symmetry and a type of mirror symmetry, the total symmetry being 5*m*. The slowly varying intensity distribution in the discs indicates that the pattern is formed by the interaction between ZOLZ reflections. Thus, the projection approximation should be applied to the analysis of the pattern. Patterns that were related to Fig. 2.5.3.26(*a*) by an inversion were observed when the illuminated specimen area was changed, indicating the existence of inversion domains. Table 2.5.3.15 shows possible pentagonal and decagonal point groups, which are constructed by analogy with the trigonal and hexagonal point groups (Saito *et al.*, 1992).

It can be seen that the point groups that satisfy the observed symmetry 5*m* in the projection approximation are 52, 5*m* and $\bar{1}0m2$. Point group 52 is a possibility because the horizontal

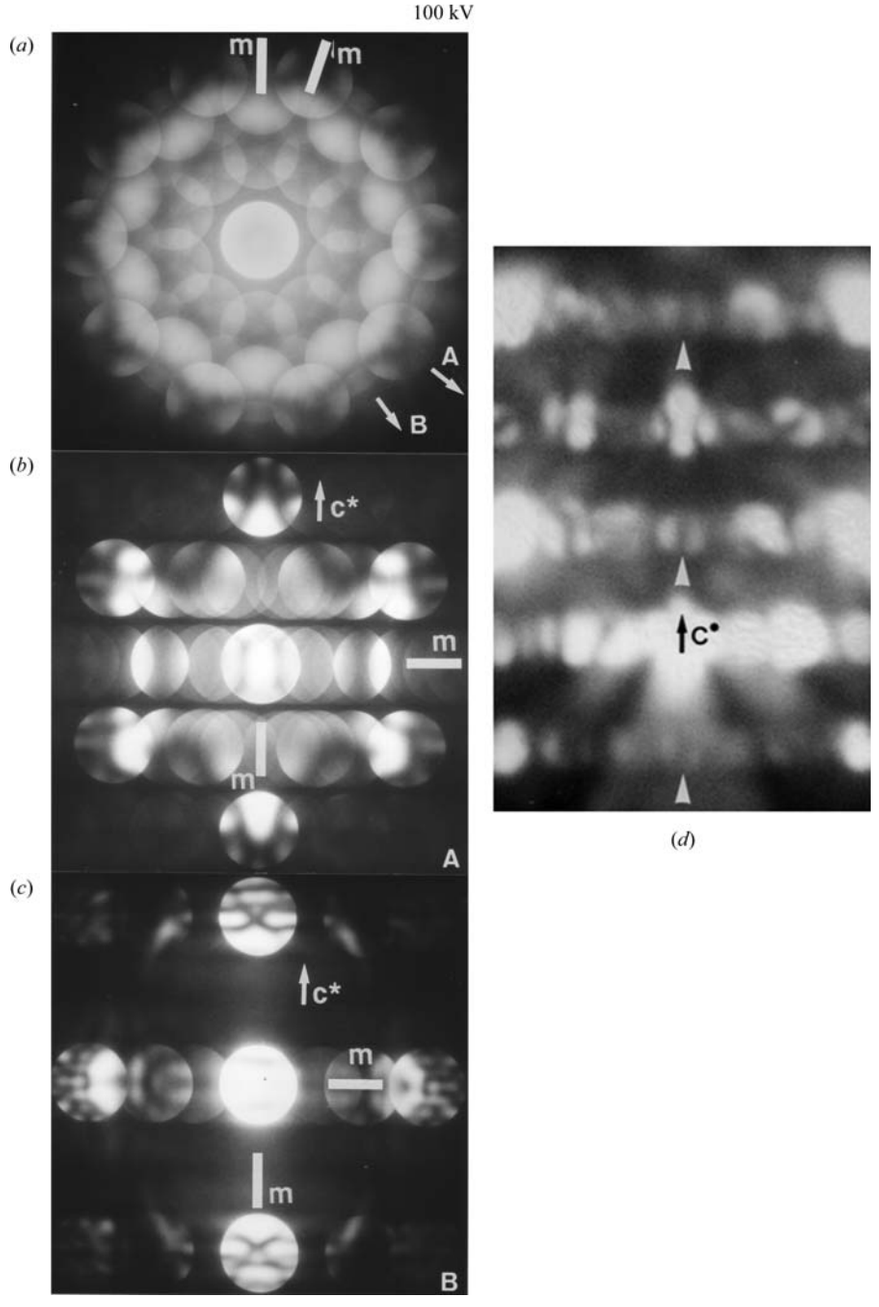

Fig. 2.5.3.27. CBED patterns of metastable $Al_{70}Ni_{20}Fe_{10}$ taken from a 3 nm diameter area. (*a*) Electron incidence along the decagonal axis: symmetry 10*mm*. (*b*) Electron incidence along direction A indicated in (*a*): symmetry 2*mm*. (*c*) Electron incidence along direction B indicated in (*a*): symmetry 2*mm*. (*d*) Reflections 00*l* (*l* = odd) show dynamical extinction lines. This alloy is determined to have the centrosymmetric space group $P10_5/mmc$.

twofold rotation axis is equivalent to the vertical mirror plane in the projection approximation. Figs. 2.5.3.26(*b*) and (*c*) were taken with beam incidences A and B, respectively, as denoted in Fig. 2.5.3.26(*a*). Mirror symmetry perpendicular to the *c* axis is seen in Fig. 2.5.3.26(*b*) and (*c*). Since the mirror symmetry requires a twofold rotation axis or a mirror plane perpendicular to the *c* axis, point groups 52 and $\overline{1}0m2$ remain as possibilities. Fig. 2.5.3.26(*c*) exhibits symmetry 2*mm*. Mirror symmetry parallel to the *c* axis requires the existence of a mirror plane parallel to the axis (a twofold rotation axis is not possible because the fivefold rotation axis already exists.). Since the mirror plane does not exist in point group 52 but does exist in $\overline{1}0m2$, the point group of the alloy is determined to be $\overline{1}0m2$. Examination of the ordinary diffraction patterns of the alloy revealed that the lattice type is primitive with a periodicity of 0.4 nm in the *c* direction and no dynamical extinction was observed. Thus, the space group of $Al_{70}Ni_{15}Fe_{15}$ was determined to be $P\overline{1}0m2$ (Saito *et al.*, 1992) by full use of the potential of CBED. This is the first quasicrystal with a noncentrosymmetric space group. High-resolution electron-microscope images revealed that the quasicrystal is composed of specific pentagonal atom clusters 2 nm in diameter (Tanaka *et al.*, 1993). Dark-field microscopy revealed the existence of inversion domains with an antiphase shift of *c*/2, the polarity being perpendicular to the *c* direction (Tsuda *et al.*, 1993).

Quasicrystals of $Al_{70}Ni_{10+x}Fe_{20-x}$ ($0 \leq x \leq 10$) were investigated by CBED and transmission electron microscopy (Tanaka *et al.*, 1993). The change in space group takes place at $x = 7.5$ upon a sudden decrease of the size of the inversion domains or a rapid mixing of the atom clusters with positive and negative polarities. As a result, the average structure becomes centrosymmetric. A CBED pattern of $Al_{70}Ni_{20}Fe_{10}$ taken at an incidence along the *c* axis shows tenfold rotation symmetry (Fig. 2.5.3.27*a*). CBED patterns taken at incidences A and B (shown in Fig. 2.5.3.27*a*) exhibit two mirror symmetries parallel and perpendicular to the *c* axis (Figs. 2.5.3.27*b* and *c*). Thus, the point group of this phase is

determined to be 10/*mmm*. Fig. 2.5.3.27(*d*) shows a CBED pattern taken by slightly tilting the incident beam to the *c** direction from incidence A. Dynamical extinction lines (arrowheads) are seen in the odd-order reflections along the *c** axis. This indicates the existence of a 10_5 screw axis and a *c*-glide plane. No other reflection absences were observed, implying the lattice type to be primitive. Therefore, the space group of $Al_{70}Ni_{20}Fe_{10}$ is determined to be centrosymmetric $P10_5/mmc$. It was found that the alloys with $0 \leq x \leq 7.5$ belong to the noncentrosymmetric space group $P\overline{1}0m2$ and those with $7.5 < x \leq 15$ belong to the centrosymmetric space group $P10_5/mmc$, keeping the specific polar structure of the basic clusters unchanged.

Another phase was found in the same alloys with $15 < x \leq 17$. This phase showed the same CBED symmetries as the phase with $7.5 < x \leq 15$. The space group of the phase was also determined to be $P10_5/mmc$. However, high-angle annular dark-field (HAADF) observations of the phase with $15 < x \leq 17$ showed that each atom cluster has only one mirror plane of symmetry (Saitoh *et al*., 1997, 1999). This implies that the structure of the specific cluster is changed from that of the phase with $7.5 < x \leq 15$. The clusters are still polar but take ten different orientations, producing centrosymmetric tenfold rotation symmetry on average, which was confirmed by HAADF observations (Saitoh, Tanaka & Tsai, 2001).

These three phases have been found for the similar alloys Al–*M*1–*M*2, where *M*1 = Ni and Cu, and *M*2 = Fe, Co, Rh and Ir (Tanaka *et al.*, 1996). Subsequently, decagonal quasicrystals were found in Al–Pd–Mn, Zn–Mg–RE (RE = Dy, Er, Ho, Lu, Tm and Y) and other alloy systems (Steurer, 2004). There are seven point groups in the decagonal system (Table 2.5.3.15). However, only two point groups, $\overline{1}0m2$ and 10/*mmm*, and two space groups, $P\overline{1}0m2$ and $P10_5/mmc$, are known reliably in real materials to date, though a few other point and space groups have been reported.

For further crystallographic aspects of quasicrystals, the reader is referred to the comprehensive reviews of Tsai (2003) and Steurer (2004), and to a review of more theoretical aspects by Yamamoto (1996).

2.5.4. Electron-diffraction structure analysis (EDSA)[2]

By B. K. Vainshtein and B. B. Zvyagin

2.5.4.1. Introduction

Electron-diffraction structure analysis (EDSA) (Vainshtein, 1964) based on electron diffraction (Pinsker, 1953) is used for the investigation of the atomic structure of matter together with X-ray and neutron diffraction analysis. The peculiarities of EDSA, as compared with X-ray structure analysis, are defined by a strong interaction of electrons with the substance and by a short wavelength λ. According to the Schrödinger equation (see Section 5.2.2) the electrons are scattered by the electrostatic field of an object. The values of the atomic scattering amplitudes, f_e, are three orders higher than those of X-rays, f_x, and neutrons, f_n. Therefore, a very small quantity of a substance is sufficient to obtain a diffraction pattern. EDSA is used for the investigation of very thin single-crystal films, of ~5–50 nm polycrystalline and textured films, and of deposits of finely grained materials and surface layers of bulk specimens. The structures of many ionic crystals, crystal hydrates and hydro-oxides, various inorganic, organic, semiconducting and metallo-organic compounds, of various minerals, especially layer silicates, and of biological structures have been investigated by means of EDSA; it has also been used in the study of polymers, amorphous solids and liquids.

Special areas of EDSA application are: determination of unit cells; establishing orientational and other geometrical relationships between related crystalline phases; phase analysis on the basis of d_{hkl} and I_{hkl} sets; analysis of the distribution of crystallite dimensions in a specimen and inner strains in crystallites as determined from line profiles; investigation of the surface structure of single crystals; structure analysis of crystals, including atomic position determination; precise determination of lattice potential distribution and chemical bonds between atoms; and investigation of crystals of biological origin in combination with electron microscopy (Vainshtein, 1964; Pinsker, 1953; Zvyagin, 1967; Pinsker *et al.*, 1981; Dorset, 1976; Zvyagin *et al.*, 1979).

There are different kinds of electron diffraction (ED) depending on the experimental conditions: high-energy (HEED) (above 30–200 kV), low-energy (LEED) (10–600 V), transmission (THEED) and reflection (RHEED). In electron-diffraction studies use is made of special apparatus – electron-diffraction cameras in which the lens system located between the electron source and the specimen forms the primary electron beam, and the diffracted beams reach the detector without aberration distortions. In this case, high-resolution electron diffraction (HRED) is obtained. ED patterns may also be observed in electron microscopes by a selected-area method (SAD). Other types of electron diffraction are: MBD (microbeam), HDD (high-dispersion), CBD (convergent-beam), SMBD (scanning-beam) and RMBD (rocking-beam) diffraction (see Sections 2.5.2 and 2.5.3). The recent development of electron diffractometry, based on direct intensity registration and measurement by scanning the diffraction pattern against a fixed detector (scintillator followed by photomultiplier), presents a new improved level of EDSA which provides higher precision and reliability of structural data (Avilov *et al*., 1999; Tsipursky & Drits, 1977; Zhukhlistov *et al*., 1997, 1998; Zvyagin *et al.*, 1996).

Electron-diffraction studies of the structure of molecules in vapours and gases is a large special field of research (Vilkov *et al*., 1978). See also *Stereochemical Applications of Gas-Phase Electron Diffraction* (1988).

2.5.4.2. The geometry of ED patterns

In HEED, the electron wavelength λ is about 0.05 Å or less. The Ewald sphere with radius λ^{-1} has a very small curvature and is approximated by a plane. The ED patterns are, therefore, considered as plane cross sections of the reciprocal lattice (RL) passing normal to the incident beam through the point 000, to scale $L\lambda$ (Fig. 2.5.4.1). The basic formula is

$$r = |\mathbf{h}|L\lambda, \text{ or } rd = L\lambda, \qquad (2.5.4.1)$$

where *r* is the distance from the pattern centre to the reflection, **h** is the reciprocal-space vector, *d* is the appropriate interplanar distance and *L* is the specimen-to-screen distance. The deviation of the Ewald sphere from a plane at distance *h* from the origin of the coordinates is $\delta_h = h^2\lambda/2$. Owing to the small values of λ and to the rapid decrease of f_e depending on $(\sin\theta)/\lambda$, the diffracted beams are concentrated in a small angular interval (≤ 0.1 rad).

Single-crystal ED patterns image one plane of the RL. They can be obtained from thin ideal crystalline plates, mosaic single-crystal films or, in the RHEED case, from the faces of bulk single crystals. Point ED patterns can be obtained more easily owing to the following factors: the small size of the crystals (increase in the dimension of RL nodes) and mosaicity – the small spread of crystallite orientations in a specimen (tangential tension of the RL nodes). The crystal system, the parameters of the unit cell and the Laue symmetry are determined from point ED patterns; the probable space group is found from extinctions. Point ED patterns may be used for intensity measurements if the kinematic

[2] Questions related to this section may be addressed to Dr D. L. Dorset (see list of contributing authors).